ON REDUCING CALL DROP OUTS BY IMPROVING BIT ERROR RATE PERFORMANCE IN A GSM MOBILE COMMUNICATIONS SYSTEM

by

SUDEEP SHARMA

Presented to the Faculty of the Graduate School of

The University of Texas at Arlington in Partial Fulfillment

of the Requirements

for the Degree of

MASTER OF SCIENCE IN ELECTRICAL ENGINEERING

THE UNIVERSITY OF TEXAS AT ARLINGTON

MAY 2008

ACKNOWLEDGEMENTS

I would like to sincerely thank my advisor Dr. Venkat Devarajan for giving me the opportunity to work with him. This thesis originated as an idea from Dr. Devarajan. I have tried to pursue it to its logical conclusion under his constant guidance. He has been an endless source of inspiration and has constantly supported me in all possible ways. I sincerely value the inputs that he has given me all the way.

I would like to acknowledge Dr. Manry and Mr. Bernard Svihel for being a part of my committee. I would like to thank all the professors from UTA, especially Dr. Liang whose course work helped me to complete my research. I am grateful to all my lab mates, friends here and back home in India for their constant encouragement and motivation.

I owe everything to my parents; they have always provided me the opportunities and have been like pillars of support for me. My parents are the primary reason for all my achievements so far. I will always remain indebted to them. I dedicate this work to them.

March 3, 2008

ABSTRACT

ON REDUCING CALL DROP OUTS BY IMPROVING

BIT ERROR RATE PERFORMANCE IN A GSM

MOBILE COMMUNICATIONS SYSTEM

Publication No. _____

Sudeep Sharma, MS

The University of Texas at Arlington, 2008

Supervising Professor: Dr. Venkat Devarajan

Call Drop Out is one of the most annoying problems in Mobile Communications. It is one of the most important Quality of Service (QoS) indicators for a mobile carrier. Over the years, many strategies have been proposed to solve the problem of call drop out. But the problem is still prevalent. One of the important reasons for call drop outs is high Bit Error Rate (BER). In general, many existing wireless systems set a threshold BER before a call is dropped.

In this work, our intent is to reduce the call drop out due to high BER. Towards that end, we simulated the overall block diagram for a typical mobile communication system and measured its BER. Thereafter, we introduced a new signal processing subsystem at the receiver section to improve the BER and thereby improve the end-to - end performance of the system. In particular, the calculation of un-mixing matrix and automated identification for distinguishing separated signals was carried out. Our simulation is valid specifically for Global Systems for Mobile (GSM), although it can be extended to a Code Division Multiple Access (CDMA). Our simulation proved that the new signal processing subsystem did indeed improve the BER. The implication of this is that the existing network will see a reduction in call drops outs.

TABLE OF CONTENTS

LIST OF ILLUSTRATIONS

LIST OF TABLES

Table Page

CHAPTER 1

INTRODUCTION

1.1 Background

Cell phones keep getting fancier. But the old problems never seem to go away. Today, you can get gadgets that let you browse the web, locate the nearest restaurant or even watch live TV. But the old problems of call drop outs remain.

Call drop-out is a measure of the ability of a mobile network to maintain a call until it is terminated. The call drop-out rate is measured as the amount of call drop-outs as a percentage of calls. The lower the percentage, the better is the QoS.

The main reasons for call drop out related to BER are:

- Transmission problem: If transmission is not perfect i.e. high BER is observed, then QoS provided is not good. When the service quality drops below a threshold the call is dropped [1].
- Hand-over: Hand-over or Handoff is the process of changing the channel associated with the current connection while a call is in progress. Hand over is initiated when the BER of serving base station increases above a certain threshold [2]. If hand-over between two sectors is not well defined, it leads to call drop outs.
- Large hysteresis value during handoff: The Received Signal Strength (RSS) measurement is one of the most common criteria to initiate a handoff. Handoff is initiated if the RSS of the new Base Station BS_2 (Refer Figure 1.1) is sufficiently stronger by a hysteresis (h) value than that of the serving Base Station (BS_1). If

hysteresis is too large, the long handoff delay can cause the signal strength to be weak which may result in a dropped-call [3]

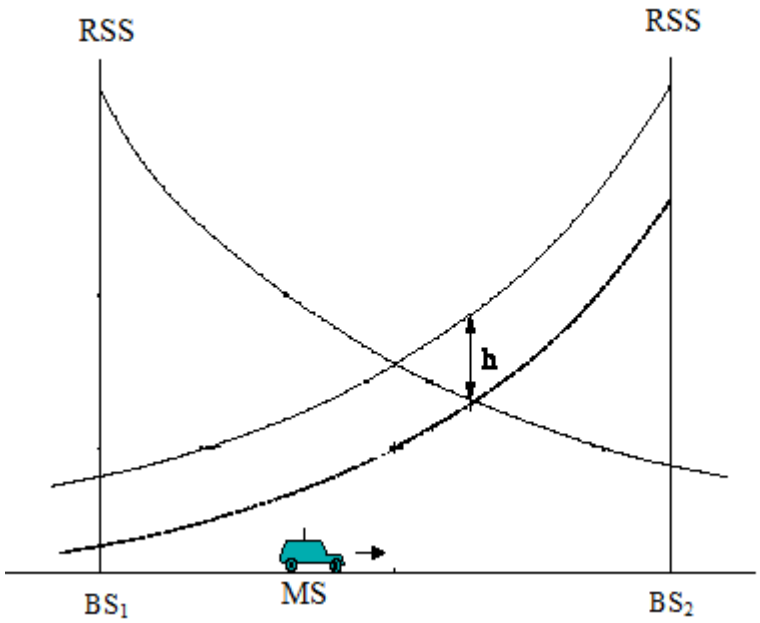

Figure 1.1 Handoff Initiation Approach

Despite the best efforts of all the carriers to reduce the call drop outs, the problem still exists and needs to be addressed.

It can be concluded from above reasons that improving BER will not only improve the overall performance of the system, but will help in reducing call drop out problem in cell phones.

1.2 Outline of the Work

In this thesis, a novel signal processing subsystem was conceptualized and developed that could be placed at the appropriate point within the receiver block diagram sequence. This subsystem was independently evaluated and validated. Thereafter, it was determined that its performance could be truly measured only if it was part of a realistic

simulation of the overall receiver. To that end, the transmitter, receiver and channel for entire mobile communication were simulated. The data which consisted of a sequence of 1's and 0's was modulated using QPSK, filtered and transmitted. The channel was simulated to introduce the effect of Ricean fading. The receiver on the other hand, consisted of a matched filter, demodulator and BER calculator. The Signal Processing Block (SPB) was introduced at the beginning of the receiver. This SPB helps to improve the BER.

The thesis is organized as follows: In Chapter 2, we provide a summary of the existing methods of call drop outs. We also discuss the connecting link between the BER and call drop out. In Chapter 3, we deal with the introduction of the anatomy of the SPB. We also describe in this chapter, the simulation performed for the stand alone validation of the SPB. In Chapter 4, we describe the physical layer modeling of a typical wireless communication system. We introduce the modeling of the SPB in the system at the end of this chapter. In Chapter 5, we present the results obtained after the simulation of entire system together. Chapter 6 provides the conclusion for the thesis and the future work required.

CHAPTER 2

TECHNIQUES FOR PREVENTING CALL DROP OUTS

This chapter provides a summary of the existing methods related to call drop outs in mobile communications. The chapter discusses with the underlying concept related to BER and call drop outs and their connectivity.

2.1 Existing Methods for Preventing Call Drop Outs

To support various integrated services with a certain QoS requirement in wireless networks, resource provisioning is a major issue. Call Admission Control (CAC) is such a provisioning strategy to limit the number of call connections into the networks in order to reduce the network congestion and call dropping [4, 5]. Various algorithms and schemes have been developed for CAC. The purpose of an admission control algorithm is to decide at the time of call arrival, whether or not a new call should be admitted into the network. Some of CAC schemes are:

- Guard Channel Schemes [5]: A portion of channel is reserved for handoff calls and whenever a channel is released, it is returned to the common pool of channels. A handoff takes place, whenever a user travels from one base station to another base station. During handoff, the user needs to release the currently allocated channel and acquire a channel from another base station without the call being dropped. The base station without Guard Channel Schemes may not have channels available, leading to call drop outs. Guard Channel schemes make sure

that a portion of channels are reserved for handoff calls and call drop outs do not occur during handoff requests.

- Queuing Priority Schemes [5]: In this scheme, calls are accepted whenever there are free channels. When all channels are busy, instead of dropping a call new calls are queued.
- Some dynamic channel assignment schemes using power control [6] have also been proposed. It is shown that these schemes reduce call dropping and increase capacity compared to those using fixed transmitter power.

2.2 Connectivity between the BER and Call Drop Outs

All the above methods speak about the call drop outs because of channel unavailability. These methods aim to improve call drop out by controlling the channel assignments. But the crux of the matter is, assuming the availability of channels, are all the new calls always admitted? What if the quality of call is not good enough? A new call is admitted if and only if its QoS constraints are satisfied without jeopardizing the QoS constraints of existing calls in the network.

QoS is usually defined according to the BER in digital transmission [1]. For example, the QoS requirement for voice users is usually expressed as a BER less than 10^{-3} in order to guarantee quality of communication.

Thus, if we improve the BER for the system, the problem of call drop out can be reduced. BER quantifies the reliability of the entire radio system from bits in to bits out. In general, the BER is the percentage of bits that have errors relative to the total number of bits received in a transmission, usually expressed as ten to a negative power. Hence BER is expressed as in equation (2.1)

$$\text{BER} = \frac{e}{N} \tag{2.1}$$

where, e = number of errors

N = total number of bits received

With a strong signal and an unperturbed signal path, this number is small and can be considered insignificant. Bit-error-rate performance is usually depicted on a two dimensional graph. The ordinate is the normalized signal-to-noise ratio (SNR) expressed as Eb/N0: the energy-per-bit (Eb) divided by the power spectral density of the noise (N0), expressed in decibels (dB). The abscissa is the BER, a dimensionless quantity, usually expressed in powers of ten. To create a graph of BER versus Eb/N0, we plot a series of points. Each of these points requires us to run a simulation at a specific value of SNR or Eb/N0. A typical plot of BER vs. Eb/N0 can be shown in Figure 2.1. If we can improve the BER curve i.e. for same Eb/N0, if we can get less BER, then we can say that we have improved the end- to-end performance of the system. This in turn will help in the reduction of call drop out.

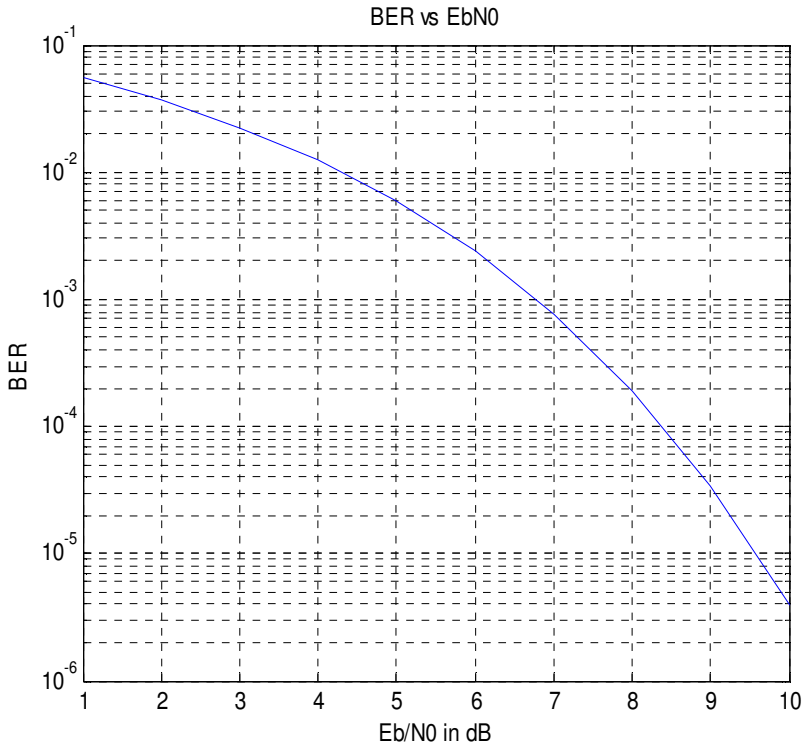

Figure 2.1 Typical plot for BER vs. Eb/N0

CHAPTER 3

ICA BASED INITIAL SIGNAL PROCESSING BLOCK

3. 1 Introduction

From Chapter 2, it is clear that we need to reduce the BER to reduce call drop outs. This chapter explains the concept behind the introduction of our new Signal Processing block (SPB). This block utilizes the concept of Independent Component Analysis (ICA). Since the underlying principle is based on ICA, it is described in greater detail below.

ICA is a technique to separate linearly mixed sources. It is a computational method for separating a multivariate signal into additive subcomponents assuming mutual statistical independence of the source signals. ICA is about performing blind source separation. It is related to other things such as entropy and information maximization, maximum likelihood density estimation and projection pursuit [7]. The inputs to ICA could come from such areas as digital images, document databases, economic indicators and psychometric measurements. In many cases, the measurements are given as a set of parallel signals or time series. Typical examples are mixtures of simultaneous speech signals that have been picked up by several microphones, brain waves recorded by multiple sensors, interfering radio signals arriving at a mobile phone, or parallel time series obtained from some industrial process. Consider the time series from two independent sources A and B as shown in Figure 3.1.

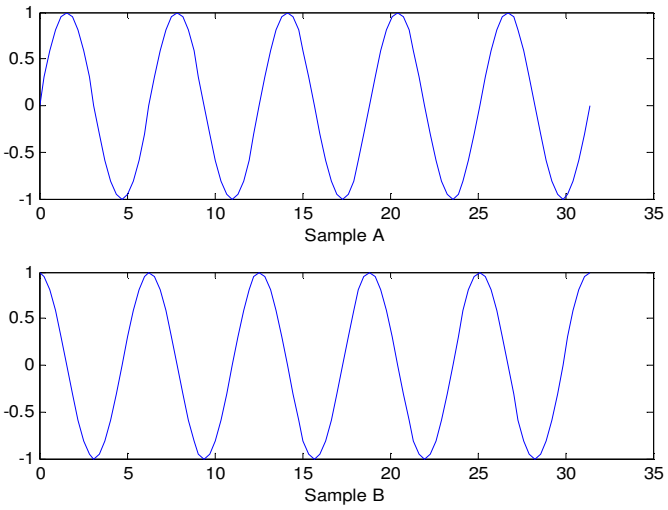

Figure 3.1 Source Signals

The independent sources are mixed linearly to get two mixtures. The mixtures obtained are 0.5A+0.7B and 1.5A-2B. These are the inputs to the ICA algorithm. At the output, we get the separated sources A and B. The mixtures or the inputs to the ICA algorithm are shown in Figure 3.2. The recovered outputs are similar to Figure 3.1.

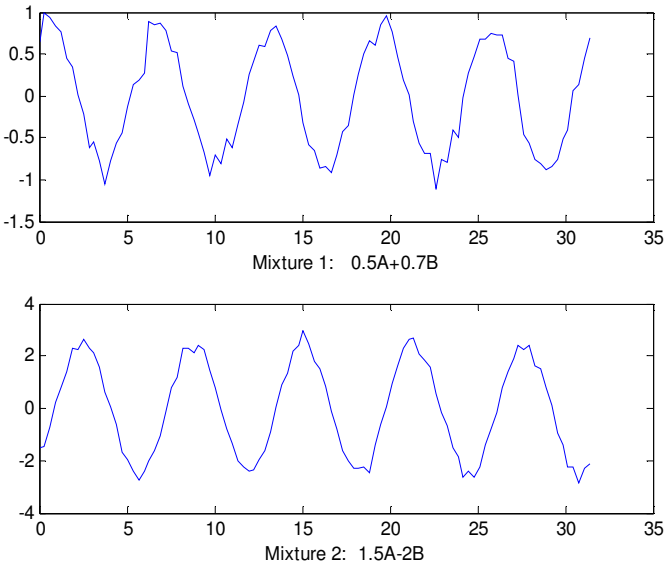

Figure 3.2 Mixture's (Inputs to ICA algorithm)

3.2 The Anatomy of our Signal Processing Block

After understanding the concept of ICA, let's examine how it can be utilized in the SPB to solve our problem. In wireless communications, when the signal is transmitted, it travels through the channel, where noise is added to the signal. Thus, received signal is a mixture of the original signal and noise. The nature of the noise added can be modeled as Additive White Gaussian Noise (AWGN) [8]. It is desirable to reduce the effect of this noise. This mixture of signal and noise when input to the SPB reduces the effect of noise.

3.2.1 The first cut at the SPB

Initially when we undertook the problem of solving call drop out, Dr. Devarajan came up with the Figure 3.3. At this stage in our development we were experimenting primarily with baseband audio.

If the voice is greater than a certain threshold i.e. if the signal is good quality, then we store the sample of voice and calculate the pitch for the stored voice. Its pitch, which corresponds to frequency with maximum amplitude, is calculated using the harmonic product spectrum (HPS) method [9]. The HPS algorithm is explained in section 3.2.2. Once the pitch is calculated it is stored for future comparison purposes. If on the other hand, the voice is less than a certain threshold i.e. if the signal quality is not good enough then it is passed through the ICA block, which gives us the separated samples of noise and voice. Even though we have a separated version of noise and voice we still need to recognize which is voice and which is noise. In this case we calculate the pitch for the separated samples and compare it with the stored pitch of the good signal. The

comparison helps in recognizing which one of the samples is voice and which one is noise.

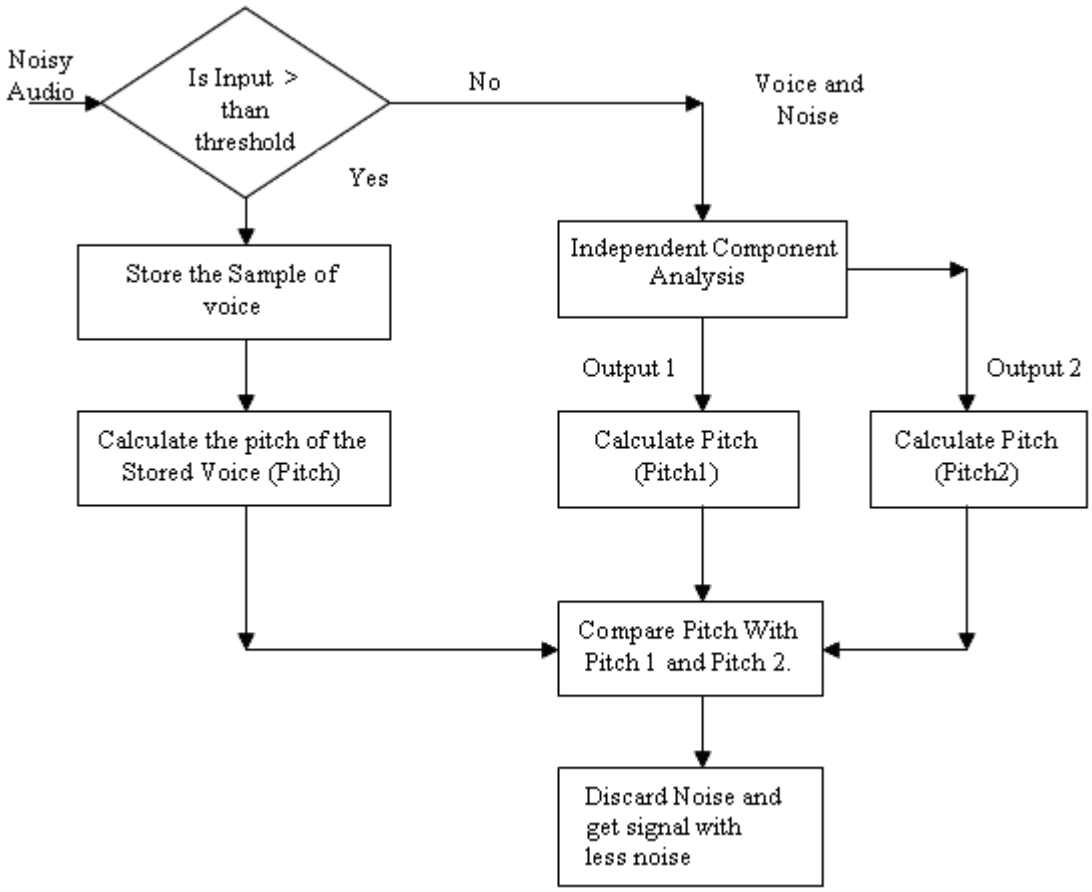

Figure 3.3 Initial block diagram of the ICA based call drop reduction system

The ICA block helps in reduction of noise using the gradient ascent rule [10]. The gradient ascent rule is explained in section 4.10.3.

We simulated a part of the block diagram using actual voice as the input. The voice was recorded and mixed with White Gaussian Noise (WGN) to get mixture 1. Mixture 2 was obtained by adding a similar type of noise to mixture 1. These mixtures,

where sent through the ICA block. The results of the experiment (shown in Figure 3.4) proved that the ICA works effectively in the separation of noise and voice.

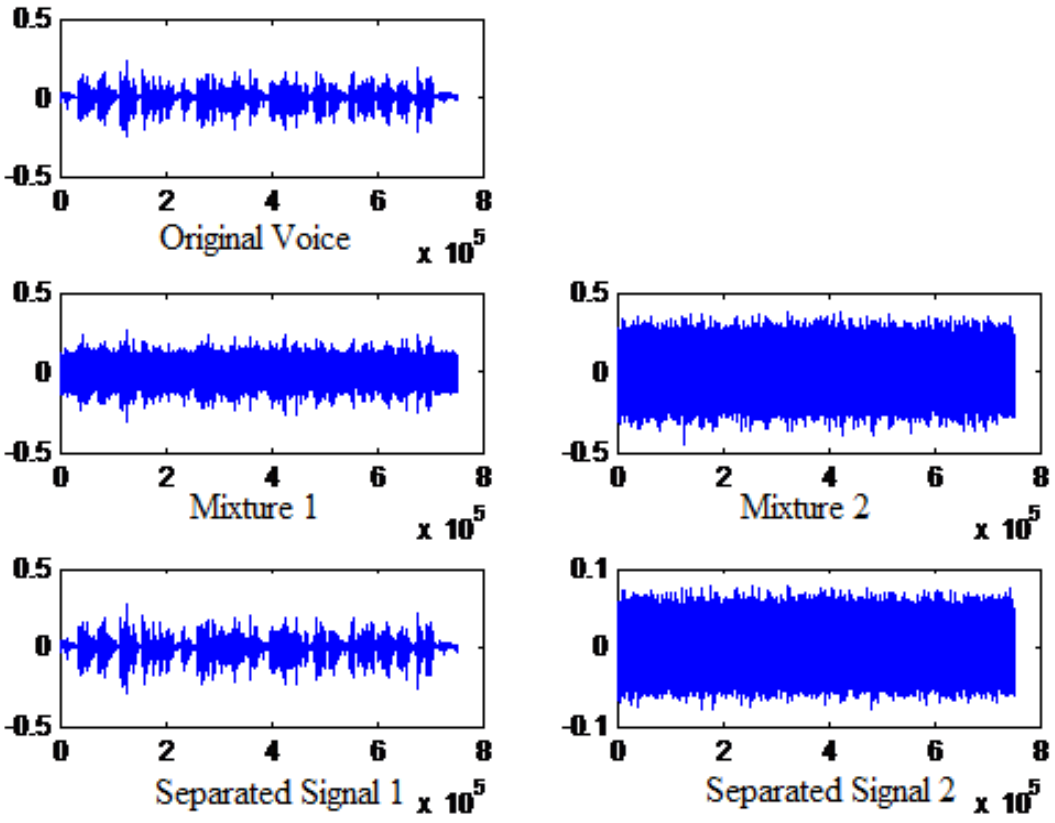

Figure 3.4 Results for Simulation of ICA

3.2.2 Harmonic Product Spectrum

As can be seen in the initial block diagram, HPS is a critical part in the automated identification of signal vs. noise after they are separated by ICA. HPS algorithm is a widely used method to calculate the pitch of speech signals. In HPS, we follow the following steps:

- Divide the input signal into segments by applying a Hanning window.
- For each window, calculate the Fourier Transform.

- Apply down sampling. In other words, compress the spectrum twice in each window by re-sampling. The first time the signal is compressed by two and then by three.
- Multiply the down-sampled version of the signals with the original signal in each window (as shown in Figure 3.5).
- Find the frequency that corresponds to the peak (maximum value). This frequency represents the dominant frequency (pitch) of that particular window. The steps described above can be diagrammatically shown as in figure 3.5

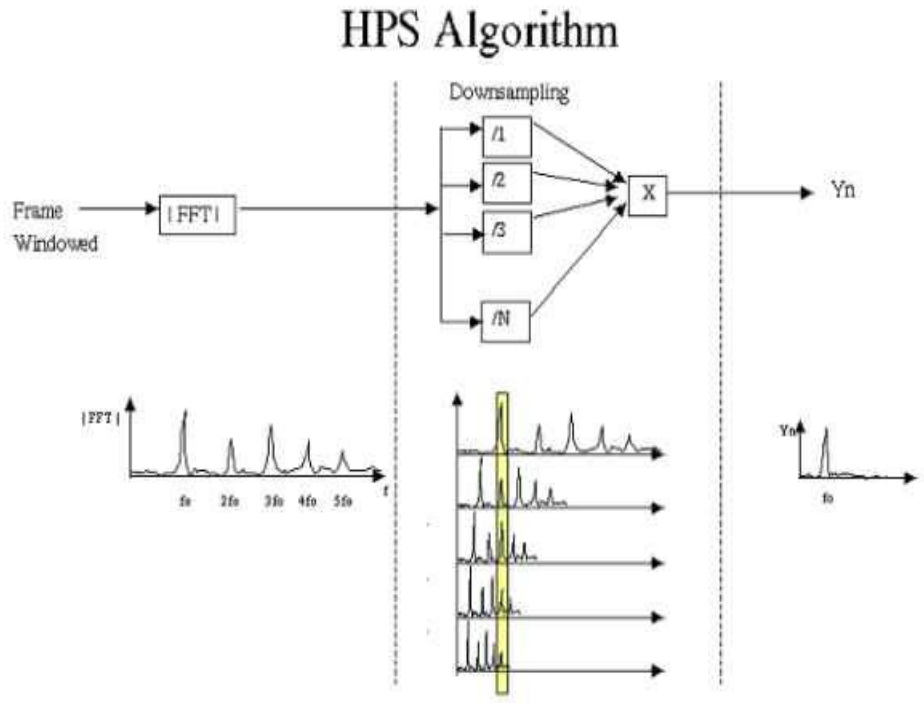

Figure 3.5 Harmonic Product Spectrum

The initial experiment was with the actual audio baseband signal. But in cell telephony/wireless world, the audio is digitalized, modulated, filtered and then

transmitted. The signal at the receiver end is a mixture of noise and data. We wanted to verify the application of our proposed block diagram in reduction of noise in a real wireless system in particular in the physical layer of such a system.

CHAPTER 4

WIRELESS COMMUNICATION SYSTEM

As discussed in previous chapter, in order to validate our proposed block, the physical layer simulation of a wireless communication system is required. In the following, we provide a brief over view of the physical layer of a wireless communication system. A simulated wireless communication system (Figure 4.1) consists of a transmitter, a receiver and a channel. The transmitter consists of a burst builder (which has the actual "payload"), modulator, up-sampler and filter. The receiver on the other hand, consists of a matched filter, down sampler, demodulator and a BER calculator. The noise added can be modeled as AWGN. The channel should take fading effects into consideration. Each block is explained briefly in the following subsections.

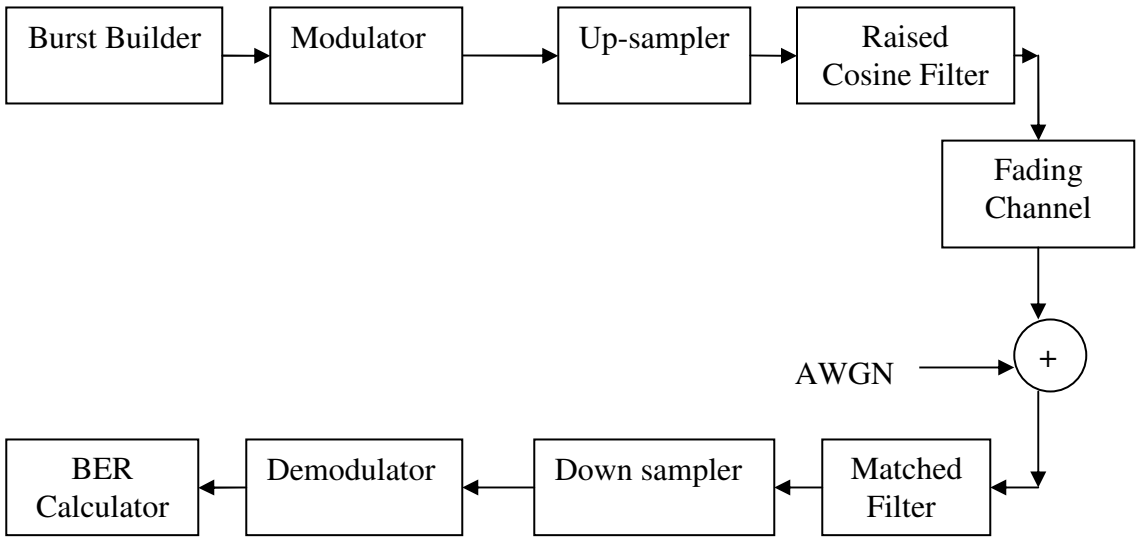

Figure 4.1 Physical Layer simulation of a wireless communication system

4.1 Burst Builder

The information or the payload (digital version of the baseband signal) transmitted at the physical layer of the communication system is in the form of bits. If voice is to be transmitted, then it is first converted to bits, modulated, up-sampled and passed through a raised cosine filter and then transmitted.

But before modulating, sometimes a burst is created. The burst consists of fixed guard bits and payload. The fixed guard bits are at the beginning and the end of the burst to avoid errors due to overlapping between the two adjacent bursts. The guard bits are discarded or removed after demodulation. The information bits coupled with guard bits are input to the modulator.

4.2 Modulator

Digital modulation maps input bits to symbols. Phase shift keying (PSK) is a popular digital modulating technique that conveys data by changing the phase of a reference signal. The general analytic expression for PSK [8] is given below.

$$s_i(t) = \sqrt{\frac{2E}{T}} \cos[\omega_0 t + \phi_i(t)] \qquad 0 \le t \le T, i = 1,....., M \tag{4.1}$$

where, the phase term $\phi_i(t)$, will have M discrete values, typically given by

$$\phi_i(t) = \frac{2\pi i}{M}, \qquad \text{i=1,....., M} \tag{4.2}$$

E is the symbol energy and T is symbol time duration for $0 \le t \le T$. The most popular and widely used form of PSK is Quadrature Phase Shift Keying (QPSK).

4.2.1 QPSK

QPSK (4-ary PSK) changes the phase of the transmitted waveform. Each finite phase change represents unique digital data. A QPSK modulated carrier undergoes four distinct changes in phase that are represented as symbols and can take on the values of 0, π/2, π, and 3π/2. The general analytic expression for QPSK is given below:

$$s_i(t) = \sqrt{\frac{2E}{T}} \cos[\omega_0 t + \frac{2\pi i}{4}] \qquad 0 \le t \le T, i = 1,2,3 \,\&\, 4 \tag{4.3}$$

Each symbol represents two bits of data. The constellation diagram of a QPSK modulated carrier is shown in Figure 4.2.

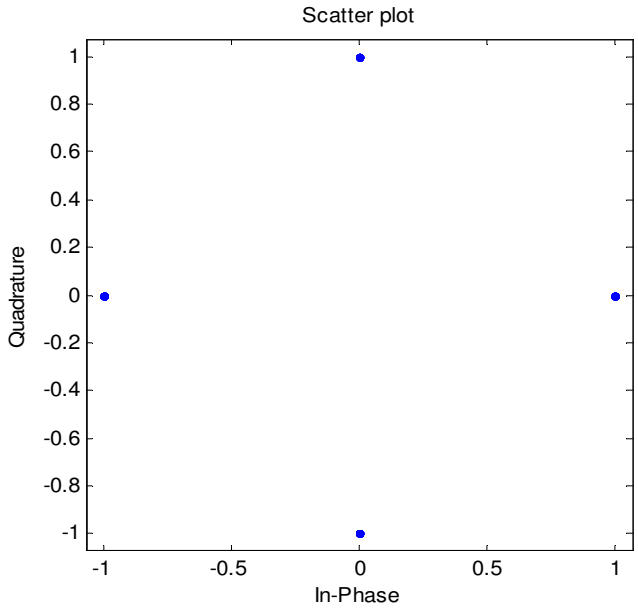

Figure 4.2 Constellation diagram for QPSK

In Table 4.1, the symbol is represented as In phase Component + j* Quadrature Component.

Table 4.1 Constellation for QPSK

Symbols	Bits	Expression	Phase	In phase	Quadrature
S_1	00	$\sqrt{\frac{2E}{T}}\cos(\omega t + 0)$	0	1	0
S_2	10	$\sqrt{\frac{2E}{T}}\cos(\omega t + \frac{\pi}{2})$	π /2	0	1
S_3	11	$\sqrt{\frac{2E}{T}}\cos(\omega t + \pi)$	π	-1	0
S_4	01	$\sqrt{\frac{2E}{T}}\cos(\omega t + \frac{3\pi}{4})$	3π /4	0	-1

Since the phase change of S_1 is 0, the expression of S_1 is $\sqrt{\frac{2E}{T}}\cos(\omega t + 0)$ and it's represented as I = 1, Q = 0 on the IQ plane. S_2 represents symbol 2 which corresponds to the bits 10. The phase change of π/2 in S_2 leads to the expression of $\sqrt{\frac{2E}{T}}\cos(\omega t + \frac{\pi}{2})$ and it's represented as I = 0, Q = 1 on the IQ plane etc.

4.3 Up-sampler and Filter

The output of the modulator is input to the up-sampler. The up-sampler inserts zeros between two symbols. Up-sampling by a factor of 16 (sampling factor) will insert 15 zeros between two adjacent symbols. Thus, up-sampling converts symbols into samples depending on the sampling factor. The length of the input after up-sampler is given as

$$l = L \times S \tag{4.4}$$

where, l = Length after up-sampling

L = Length of the symbols and

S = Sampling factor.

The output of the up-sampler is input to the pulse shaping filter. Pulse shaping filter is a raised cosine filter required to generate a smoothened waveform. Sampling in time domain results in a periodic signal in frequency domain. The filter acts as a low pass filter which will just keep a copy of the signal. The filtering is carried out to reduce the effect of Intersymbol Interference. The raised cosine filter can be expressed as

$$H(f) = 1 \qquad \text{for } |f| < 2W_0 - W$$

$$= \cos^2\left(\frac{\pi}{4}\frac{|f| + W - 2W_0}{W - W_0}\right) \qquad \text{for } 2W_0 - W < |f| < W \qquad (4.5)$$

$$= 0 \qquad \text{for } |f| > W$$

where, W is the absolute bandwidth and W_0 = 1/2T represents the minimum Nyquist bandwidth for the rectangular spectrum and -6 dB bandwidth for the raised cosine spectrum. The difference $W - W_0$ is termed as excess bandwidth. The raised cosine filter is implemented using code provided by reference [11]. The signal is ready to be "transmitted" at this time.

4.4 Channel

The transmission path between transmitter and the receiver can vary from simple line-of-sight to one that is obstructed by buildings, mountains and passing vehicles. The medium between the transmitter and receiver severely impacts the performance of the system and needs to be taken into consideration during simulation. Radio waves propagate from a transmitting antenna and travel through free space undergoing

absorption, reflection, refraction, diffraction and scattering. They are greatly affected by the ground terrain, the atmosphere, and the objects in their path, such as buildings, bridges, hills and trees. These multiple physical phenomena are responsible for the characteristic features of the received signal.

In wireless communications the channel is often modeled by a random attenuation (fading) of the transmitted signal, followed by additive noise.

4.4.1 Fading Channel

In most mobile systems, the height of the mobile antenna may be smaller than the surrounding structures. Thus, it is highly unlikely that there is a line-of-sight (LOS) path between the transmitter and receiver. Signal propagation comes from reflection and scattering from the buildings and diffraction over or around them. Thus, in practice, the transmitted signal arrives at the receiver via several paths creating a multipath situation. At the receiver, these multipath waves with randomly distributed amplitudes and phases combine to give a resultant signal that fluctuates in time and space. Therefore, a receiver at one location may have a signal that is much different from a signal at another location only a short distance away because of the change in phase relationship among the incoming radio waves. This situation causes significant fluctuations in the signal amplitude called fading which is used to describe the rapid fluctuations of the amplitudes, phases or multipath delays of a radio signal over a short period of time. Many physical factors in the radio propagation channel influence fading. More specifically, fading is caused by:

- Multiple versions of the transmitted signal that arrive at the receiving antenna, displaced with respect to one another in time and spatial orientation [12].

- Due to the relative motion between a mobile and the base station, each multipath wave experiences an apparent shift in the frequency. This effect is known as Doppler shift [12]. The Doppler shift is directly proportional to the velocity and direction of motion of the mobile with respect to the direction of arrival of the received multipath wave. The concept can be explained below:

  Consider a mobile moving at a constant velocity v, along a path segment having length *d* between points X and Y, while it receives signals from a remote source S as shown in the Figure 4.3. The difference in the path lengths traveled by the wave from S to mobile between X to Y is $d\cos\theta = v\Delta t\cos\theta$, where Δt is the time required for mobile to travel from X to Y. The apparent change in the frequency or Doppler shift is given by

$$f_d = \frac{v}{\lambda}\cos\theta \tag{4.6}$$

Doppler shift is one of the factors we need to consider while channel modeling.

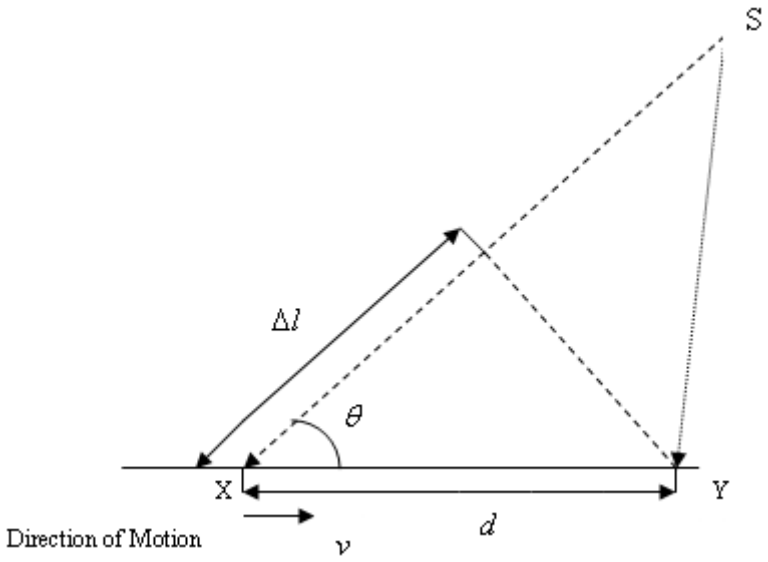

Figure 4.3 Illustration of Doppler Shift

After studying the causes of fading, next we will concentrate on Rayleigh and Ricean fading and consider the implementation of fading using Jakes model [13].

4.4.2 Rayleigh Fading

In propagation of radio waves, the fading caused by multiple paths in the absence of line of sight or direct component is approximated by Rayleigh distribution. It means that when a radio signal passes through a communication channel, the power of the signal will vary according to Rayleigh distribution. The probability density function of the received signal envelope *f(r)* for Rayleigh fading is [12].

$$f(r) = \frac{r}{\sigma^2} \exp\left\{-\frac{r^2}{2\sigma^2}\right\}, r \geq 0 \qquad (4.7)$$

where, $2\sigma^2$ is the average power. Figure 4.4 shows the effect of Rayleigh fading and over a period of 1 second with a maximum Doppler shift of 10Hz.

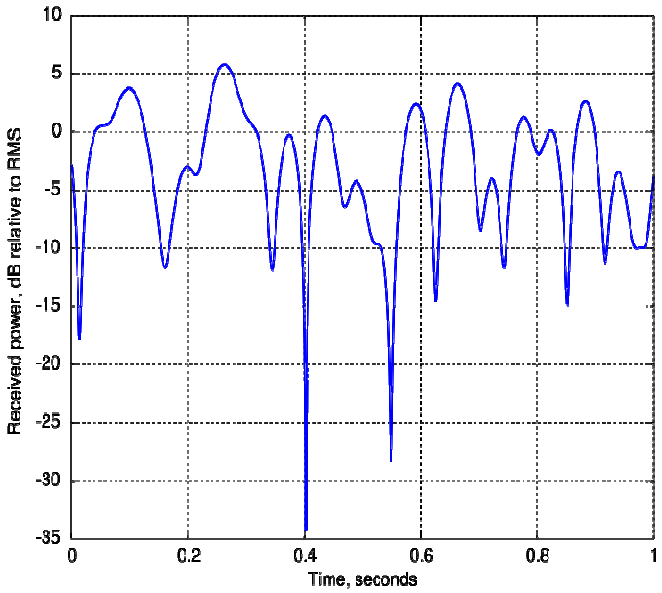

Figure 4.4 Rayleigh Fading

4.4.3 Ricean Fading

Ricean distribution [12] is observed when, in addition to multipath components, there also is a direct path between the transmitter and receiver. In such a situation, the multipath components are superimposed on a stationary dominant signal. Ricean distribution is given by

$$f(r) = \frac{r}{\sigma^2} \exp\left\{ -\frac{r^2 + k_d^2}{2\sigma^2} \right\} I_o\left(\frac{r k_d}{\sigma^2} \right), r \geq 0 \tag{4.8}$$

where, $I_o\left(\frac{r k_d}{\sigma^2} \right)$ is the zeroth-order modified Bessel function of the first kind.

Ricean distribution is often described in terms of the Ricean factor *K*, defined as the ratio between the deterministic signal power (from the direct path) and the diffuse signal power (from the indirect paths). *K* is usually expressed in decibels as

$$K(dB) = 10 \log_{10}\left(\frac{k_d^2}{2\sigma^2} \right). \tag{4.9}$$

If k_d goes to zero, the direct path is eliminated and the envelope distribution becomes Rayleigh; with K = ∞ the channel does not exhibit any fading at all. Doppler shift and the Ricean factor are used to specify Ricean fading.

4.4.4 Channel modeling using Jakes Model

The fading signal results from interference between several scattered signals and the direct signal where it exists [14]. A complex model of the received signal can be specified by equation (4.10)

$$r(t) = g(t)s(t)+n(t) \tag{4.10}$$

where, *s(t)* = transmitted signal.

$g(t)$ = fading coefficient.

$n(t)$ = noise added.

For Rayleigh fading, $g(t)$ is modeled as a complex Gaussian random process [12]. The overall fading coefficient is a complex envelope with in-phase and quadrature components. Thus, the coefficient in terms of in-phase and quadrature components [20] is given by

$$g(t)= g_I(t)+jg_Q(t) \tag{4.11}$$

This coefficient when multiplied by the transmitted signal simulates the effect of fading. A useful fading channel simulator suggested by Jakes is based on the sum of sinusoids [13]. Jakes model gives the in-phase and quadrature components of the fading coefficient, which helps in the simulator design of a Rayleigh fading channel.

The parameters used in Jakes model are defined as follows:

N = Number of sinusoids (number of paths). If there are M low frequency oscillators to generate these sinusoids then,

$$M = \frac{1}{2}(\frac{N}{2}-1) \tag{4.12}$$

The frequency for each oscillator is given by

$$\omega_n = \omega_m \cos\frac{2\pi n}{N} \quad , \text{n = 1, 2, ….., N} \tag{4.13}$$

The in-phase and quadrature components for the channel coefficient are defined by Jakes as

$$g_I(t) = \sqrt{2}\left\{2\sum_{n=1}^{M}\cos\beta_n \cos\omega_n t + \sqrt{2}\cos\alpha\cos\omega_m t\right\} \tag{4.14}$$

$$g_Q(t) = \sqrt{2}\left\{2\sum_{n=1}^{M} \sin\beta_n \cos\omega_n t + \sqrt{2}\sin\alpha\cos\omega_m t\right\} \tag{4.15}$$

where, α and β_n are the model parameters defined as

$$\beta_n = \frac{\pi n}{M} \tag{4.16}$$

$$\alpha = 0 \tag{4.17}$$

Thus, channel coefficient is $g(t) = g_I(t) + jg_Q(t)$. The Jakes simulator is shown in the Figure 4.5

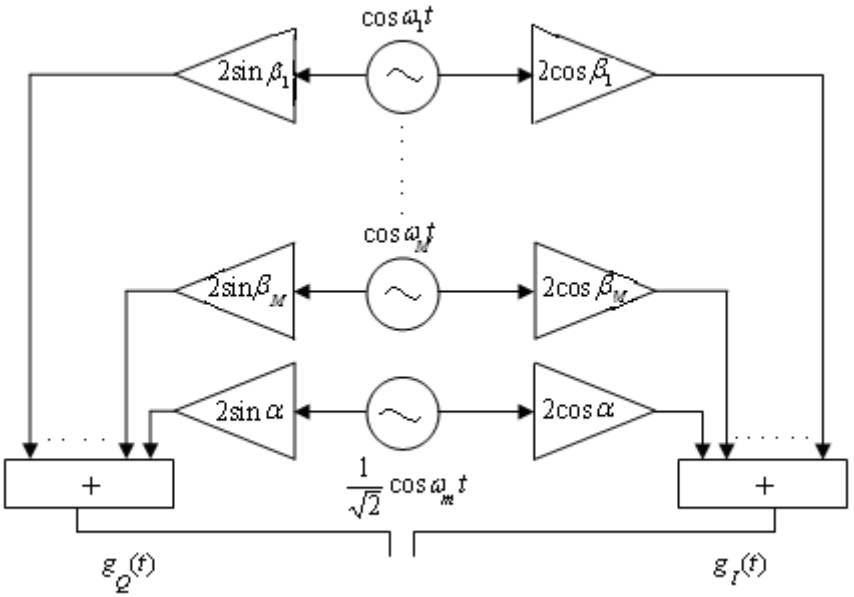

Figure 4.5 Jakes Model [13]

The channel should not change the magnitude of the transmitted signal. To ensure this, we need to normalize the in-phase and quadrature components of the coefficient, which will normalize the magnitude. This is achieved as defined in [13].

$$g_I'(t) = \frac{g_I(t)}{\sqrt{M+1}} \quad \text{and} \quad g_Q'(t) = \frac{g_Q(t)}{\sqrt{M}} \tag{4.18}$$

To implement Ricean fading, it is important to consider the fading factor K and the Doppler shift. The Ricean fading channel can be implemented as shown in Figure 4.5. As the value for K increases, the effect of fading reduces. Ricean factor K in dB is given as follows

$$K = 10\log\frac{1}{A^2} \tag{4.19}$$

The direct path power is assumed to be 1 and the scattered path power is assumed to be A^2. The factor B is present to normalize the magnitude of the total gain.

$$B = \frac{1}{\sqrt{1+10^{-K/10}}} \tag{4.20}$$

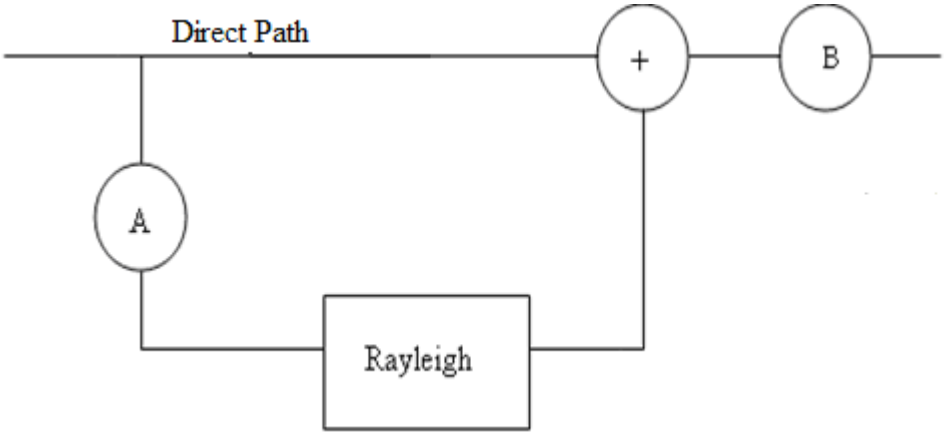

Figure 4.6 Ricean Fading Simulation

When the signal travels through the channel, WGN is added.

4.5 AWGN

The AWGN [8] is noise with a constant spectral density and a Gaussian distribution. If the transmitted signal *s(t)* is disturbed by a simple WGN *n(t),* then the received signal *r(t)* is given by

$$r(t) = s(t) + n(t) \tag{4.21}$$

Equation (4.21) can be treated as the mathematical model for an AWGN channel. In this model, the signal to noise ratio (SNR) is one of the important factors. It is important to control the amount of noise added in terms of noise power to obtain the desired simulated SNR. If the signal power is known and desired SNR is known, then it is easy to determine the amount of noise to be added.

For a random variable, signal power is equal to its mean-squared value. The signal power thus equals E [S^2] = variance of signal for zero mean [15]. Once we have the signal power, the noise power in dB is given by,

$$\text{Noise} = \text{SNR} - \text{Signal Power in dB.} \tag{4.22}$$

Even though we calculated noise power using the desired SNR, the performance of the wireless communication system is always measured in terms of bit error rate (BER) with different values of Eb/N0, where Eb is the bit energy of a signal and N0 is the noise power spectral density for WGN. Thus, we need to find a relation between SNR and Eb/N0.

Eb/No is a measure of signal to noise ratio for a digital communication system. The relation between SNR and Eb/N0 is given as in [16]

$$\text{SNR} = \text{Eb/N0} + 10\log_{10}(k) \tag{4.23}$$

where, k = number of bits per symbol. For any M-ary modulation, the relation between the number of bits and symbols is given as

$$k = \log_2(M) \tag{4.24}$$

Thus, for QPSK i.e., 4-PSK

$$k = \log_2(4) = 2 \tag{4.25}$$

Therefore, from equation (4.23), $SNR = Eb/N0 + 10\log_{10}(2) = Eb/N0+3$. (4.26)

From equation (4.22), Noise in dB is given as

$$Noise = Eb/N0 + 10\log_{10}(k) - \text{Signal Power in dB}. \tag{4.27}$$

From equation (4.26) for QPSK,

$$Noise = Eb/N0+3 - \text{Signal Power in dB}.$$

After addition of noise, the signal is input to a matched filter and down-sampler.

4.6 Matched Filter and Down-sampler

The receiver section consists of a matched filter and a down-sampler. A matched filter is an optimal filter for maximizing the SNR in the presence of AWGN [11]. If *h(t)* is the impulse response of a matched filter, then its output is given as a convolution of received signal and its impulse response.

$$M_{filter}(t) = R(t) * h(t) \tag{4.28}$$

where, *R(t)* = Received signal at the input of a matched filter.

h(t) = Impulse response of a matched filter.

$M_{filter}(t)$ = The output of a matched filter.

Thus, from the above discussion it is clear that *h(t)* is chosen such that SNR at the output of the filter is maximized which in turn, helps in minimizing the BER.

At the transmitter end, up-sampling is carried out before the data is input to a pulse shaping filter. Analogously, at the receiver end, down-sampling is carried out after filtering. Down-sampling by a factor of 16 describes the process of keeping every 16^{th} sample and discarding the rest. Note that the sampling factor at the transmitter and the receiver section should be the same. After down-sampling by a factor of *S,* the length of the output samples is given as

$$l = \frac{M}{S} \tag{4.29}$$

where, M = Length at the output of a matched filter.

S = Sampling factor.

The output of a down-sampler is input to a demodulator where, symbols are converted back to bits.

4.7 Demodulator

Digital demodulation is the act of converting symbols back to bits. Since we have implemented QPSK modulation, we will see how the QPSK demodulation is carried out.

4.7.1 QPSK Demodulation

In case of the QPSK demodulation (Figure 4.7), the symbol to bit mapping is accomplished using hard-slicer detection where, the received symbols are converted to bits according to the phase of the received signal. The angle for each symbol is calculated and the decision is made as per the calculated angle.

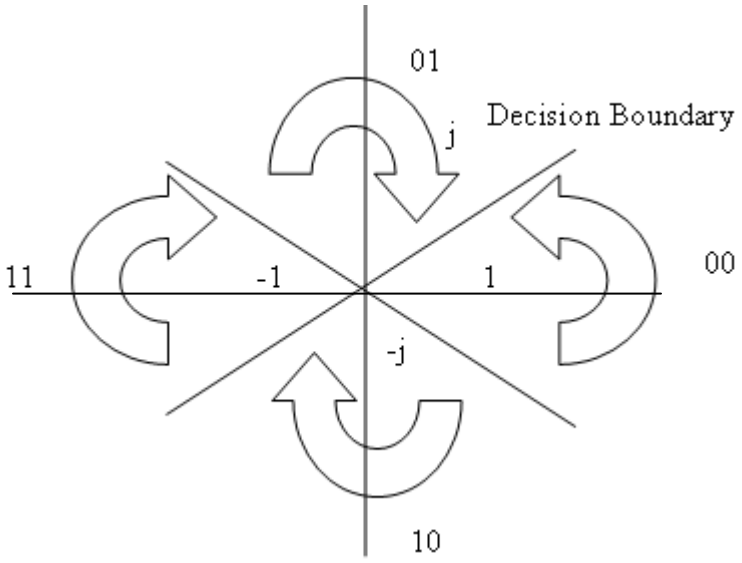

Figure 4.7 Hard Slicer Detection

For QPSK demodulation, the decision table is shown below, which gives the relation between the calculated angle and the detected symbols.

Table 4.2 Decision table for QPSK Demodulation

Range of Angle Calculated	Detected Symbol	Converted Bits
$\pi/4$ to $-\pi/4$	1	00
$\pi/4$ to $3\pi/4$	j	01
$3\pi/4$ to $-3\pi/4$	-1	11
$-3\pi/4$ to $-\pi/4$	-j	10

4.8 Probability of Error

Probability of error is defined as the probability that the transmitted symbol is detected in error. This error is largely influenced by the channel conditions. Channel fading and AWGN causes this error. Probability of error is often expressed as probability

of bit error (same as BER) or probability of symbol error. The BER calculator is used to compare the actual payload with the decoded bits. The error introduced depends on the value of the SNR. Higher value of the SNR indicates that less noise is added and fewer errors are introduced.

Since, we are dealing with the improvement of the BER, it is important that we know the BER for the existing QPSK modulation. The symbol error rate for the QPSK modulation with AWGN channel [8] is given as in equation (4.30)

$$P_M = 2Q(\sqrt{2Eb/N_0})[1 - 2Q(\sqrt{2Eb/N_0}] \tag{4.30}$$

As per the relation between the BER and symbol error rate [8] we have

$$P_b = \frac{1}{k} P_M \tag{4.31}$$

where, P_b = Bit error rate

P_M = Symbol error rate and

k = number of bits per symbol

Hence, for QPSK (4-ary PSK), M = 4. Therefore, k = 2.

$$\text{Bit Error Rate} = \frac{1}{2} P_M \tag{4.32}$$

Thus, the BER for QPSK with the AWGN channel is given as in equation (4.33)

$$P_b = Q(\sqrt{2Eb/N_0})[1 - 2Q(\sqrt{2Eb/N_0}] \tag{4.33}$$

Hence, from equation (4.33) it can be seen that the probability of bit error or the BER is dependent on the ratio of energy per bit to noise spectral density.

The plot for the BER vs. Eb/N0 using equation (4.33) was implemented (Figure 4.8). The curve can be treated as the theoretical baseline curve.

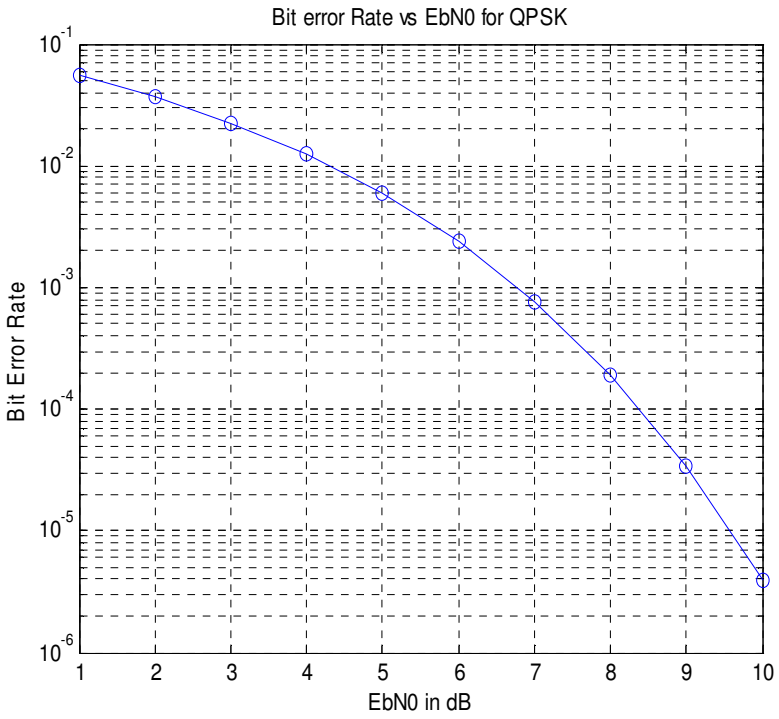

Figure 4.8 Theoretical BER curve for QPSK

4.9 Signal Processing Block incorporated in the physical layer

4.9.1 Overview and justification

Now that we have established the flow of signal through a wireless receiver, we can define the introduction of our ICA based Signal Separation and Identification block which henceforth we call the Signal Processing Block (SPB). The SPB is introduced in the signal flow as shown in Figure 4.9.

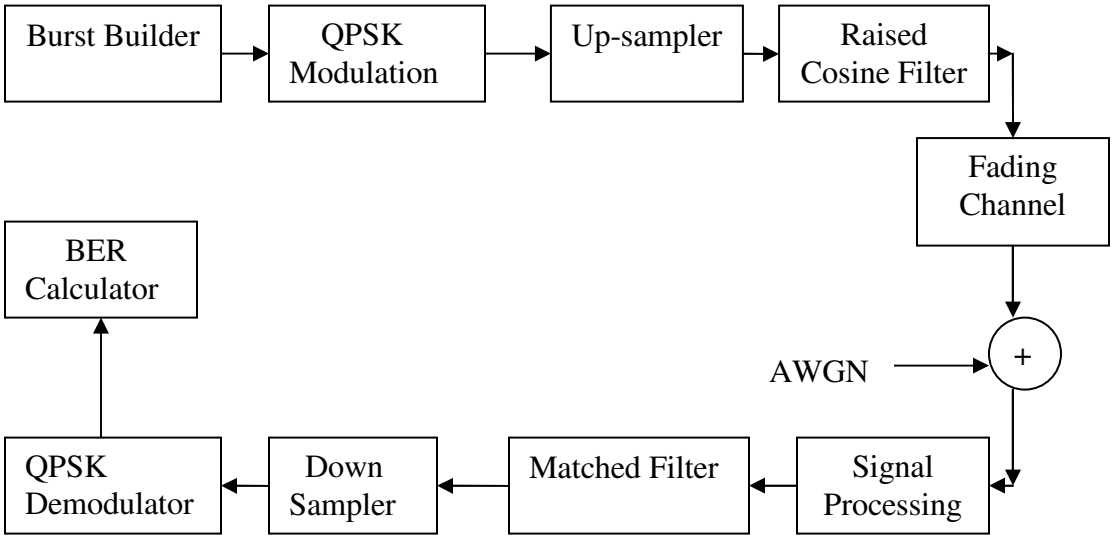

Figure 4.9 Physical layer wireless communication system with the SPB

A decision boundary needs to be defined for the mapping purpose at the demodulator. Based on the decision boundaries, the detector decides what the received symbol is and accordingly, converts that symbol into bits. The detection process can go wrong in the presence of noise. Hence, the noise reduction blocks are always placed before the demodulator of the receiver section of a wireless system, preferably at the beginning of the receiver. Our SPB is a noise filtering block. Therefore, it should be placed at the beginning of the receiver section. The next section, describes the details of each sub-blocks of the SPB.

4.10 Detailed description of the SPB

In this section, we describe the modification of our initial implementation of the ICA based system (Figure 3.3). The modifications (Figure 4.10) were necessitated by the fact that we are dealing with digital steams rather than analog. Further, in a real wireless

system digital streams have already been modulated, up-sampled and filtered. Also, the pitch detection scheme used in the earlier block diagram is no longer viable in this scenario. For these reasons we developed the new SPB block shown in the figure 4.10. In this block diagram the middle two blocks represents the ICA. The pitch based signal and noise separator in the Figure 3.3 has been replaced by an auto-correlation based identification block. Each block is explained further in the following sections.

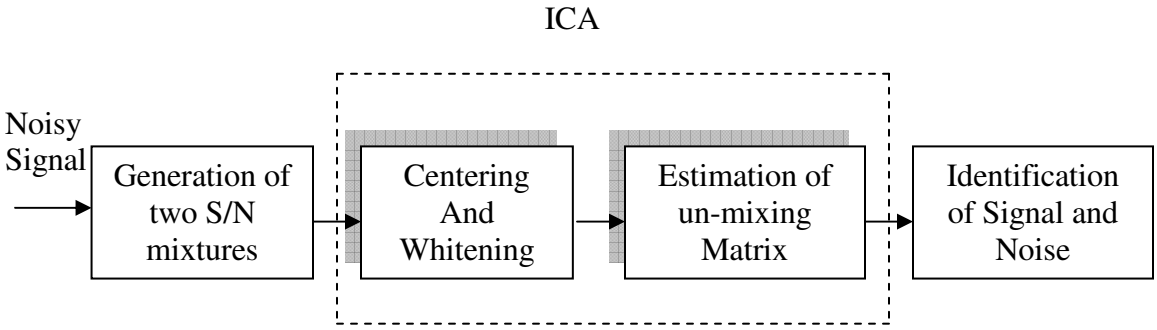

Figure 4.10 Signal Processing Block

4.10.1 Generation of two Signal and Noise Mixtures

The input at the receiver section of a wireless communication system is a mixture of noise and data. Since we are trying to reduce the effect of noise from the actual data, we require two mixtures. The fact that the noise added in a wireless communication system is modeled as AWGN is used to generate another mixture. The mixture of signal and noise is first input to this block wherein another mixture is generated [11]. Now there are two mixtures which can be represented in matrix form as follows:

$$X = AS \tag{4.34}$$

where, X = signal mixture

S = Source Signal or pure signal

A = mixing matrix

After this, the mixture is input to the next sub-block for centering and whitening.

4.10.2 Centering and Whitening

The generated mixtures are input to the next sub-block, where centering and whitening are performed. Centering and whitening are prior steps implemented to simplify the calculation of an un-mixing matrix [11]. Centering a vector X means calculating its mean and subtracting it from the vector X. Whitening is performed to transform the observed vector X so that we obtain a new vector whose components are uncorrelated.

4.10.3 Estimation of Un-mixing Matrix

The two mixtures using equation (4.34) can be expressed as:

$$X_1 = aS_1 + bS_2 \tag{4.35}$$

$$X_2 = cS_1 + dS_2 \tag{4.36}$$

where, $A = \begin{bmatrix} a & b \\ c & d \end{bmatrix}$ is the mixing matrix. S_1 is our signal and S_2 is noise (We treat each of these as two separate "sources"). Our task is to estimate matrix S, without any knowledge of A. We assume that A is an invertible matrix, then

$$S = A^{-1}X = WX \tag{4.37}$$

From equation (4.37), it is clear that we need to determine W to estimate S where, W is the un-mixing matrix. This problem of finding W is called a blind source separation problem [11], since we need to separate the sources without any knowledge of W.

Gradient ascent rule [18] is an optimization method that maximizes a function of multiple parameters by iteratively improving an initial guess using the gradient, which points in the direction of maximum slope. According to the rule, the un-mixing matrix W is given as:

$$W(k+1) = W(k) + l[I - f(y(k))y^T(k)]W(k) \tag{4.38}$$

where, $f(y(k))$ is a mathematical function that produces a sigmoid curve, a curve having an "S" shape. Often, a sigmoid function refers to the special case of the logistics function defined by the equation (4.40)

$$Y(k) = 1/(1-e^{-k}) \tag{4.39}$$

The characteristics of logistics function is shown in figure 4.11

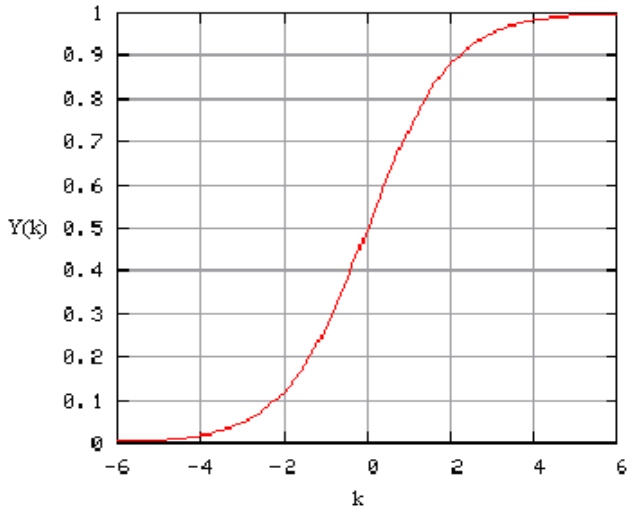

Figure 4.11 Logistics function

l is the learning rate which is typically chosen to be 0.001 [18]. This gradient based algorithm is used for the estimation of W.

For the actual simulation, we consider the system depicted in Figure 4.12, where a column vector *S* denotes two signal sources, *X* denotes the two mixtures, while the column vector *U* denotes the two separated signals, and *Y* denotes the intermediate iterative output.

$$X=AS \tag{4.40}$$

$$U = WX \tag{4.41}$$

$$Y = G(U) \tag{4.42}$$

where, A and *W* are 2 by 2 matrices, representing the mapping from *S* to *X* and from *X* to *U,* respectively, and *G(U)* is a non-linear mapping from *U* to *Y.*

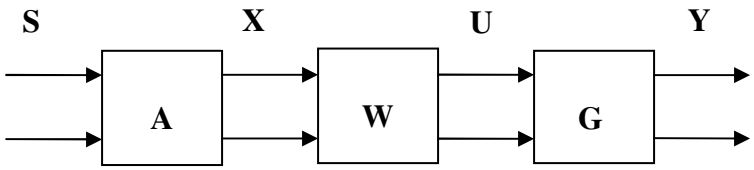

Figure 4.12 Simulation using gradient ascent rule

Initially, we assume a random value for *W* matrix and then use the gradient ascent rule during iterations. The discrete form of the gradient ascent rule for calculating *W* based on equation (4.38) is given by equation (4.43).

$$W_{new} = W_{old} + l[I - \frac{2}{1+e^{-u}} u^{'}]W_{old} \tag{4.43}$$

Thus, using the above rule the sources can be separated. In other words, mixing matrix *W* can be calculated, if the sources are independent. One of the seperated sources will have the actual signal with very little noise (henceforth called simply as signal) and

the other source will be mostly noise (henceforth called as noise). The sepearted sources are then input to the next sub-block for the identification between the signal and noise.

4.10.4 Identification of Signal and Noise

The basis of our identification algorithm is the following:

The noise added in a communication system is WGN, so the separated noise is similar to WGN. It will have some characteristics different from the other separated signal. We utilize the autocorrelation characteristics of each of these for the identification purpose.

Noise is highly uncorrelated. Autocorrelation is the correlation of a signal with itself [19]. We can therefore represent the autocorrelation function of noise as

$$R_{XX}(n, n+m) = \sigma^2 \delta[m]. \quad (4.44)$$

We use this characteristic for the identification of the noise signal.

The signal on the other hand, will have an auto-correlation function with some significant width about *m*. In our signal the original payload was likely un-correlated because in real wireless systems this is the output of a companding codec. In any case, the stream of zeros and ones would be un-correlated. However, the up-sampling of this un-correlated stream by some factor (in our case 16) introduces correlation within this bit stream, which would help identify it as being different from noise.

All the above sections explain the necessary blocks, for the physical layer simulation of a wireless communication system. Often, depending on the applications, channel coding and decoding techniques are employed to further improve the BER. We have implemented channel coding in our simulation of a realistic wireless system.

Therefore, in the next two sections we describe a commonly used channel coding and decoding technique.

4.11 Channel Coding

Channel coding refers to the class of signal transformations designed to improve the communications performance by enabling the transmitted signals to better withstand the effects of various channel impairments such as noise, interference and fading [8]. Channel coding adds the redundant bits which can be used for the detection and correction purposes at the receiver end. Convolution coding is one of the most common channel coding techniques, used to detect and correct the errors and thereby improve the performance. A convolutional encoder operates on the incoming message sequence continuously in a serial manner. A convolutional code is described by three integer's *n*, *k* and *L*. Convolution encoder is often described as an *(n,k)* encoder.

where, n = number of output bits against each input shift.

k = number of bits shifting from the source to encoder at a time.

L = constraint length which is defined as the number of shifts over which a single message bit can influence the encoder output.

$$\text{Code rate} = \frac{k}{n} \tag{4.45}$$

4.11.1 Example

The encoder of a convolution code has a memory. It consists of the shift registers as shown in Figure 4.13. It is a (2, 1) encoder with a constraint length of 3 and code rate of ½. At each input bit time, a bit is shifted in to the left most stage (S_1) and the bits in the register are shifted one position to the right (S_1 and S_2). Next, the output switch samples

the output of each modulo-2 adder and forms the code word associated with the bit just inputted. The sampling is repeated for each input bit. L-1 zero bits are appended to the end of the input sequence, for the purpose of clearing or flushing the encoding shift registers of the data bits. From the Figure 4.10, it can be seen that $C_1 = S_1 \oplus S_2 \oplus S_3$ and $C_2 = S_1 \oplus S_3$.

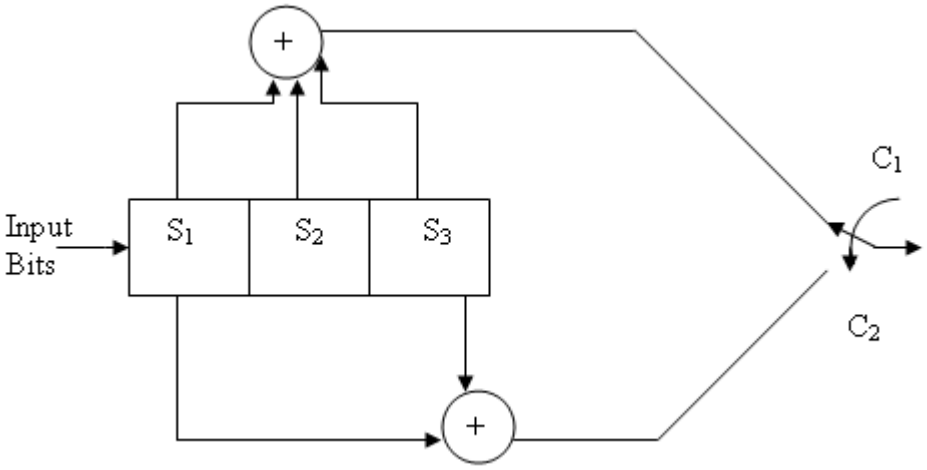

Figure 4.13 Convolution Encoder

For Message bits 110 we consider following table 4.3

Table 4.3 Illustration for convolution coding

S_1	S_2	S_3	C_1	C_2
0	0	0		
1	0	0	1	1
1	1	0	0	1
0	1	1	0	1
0	0	1	1	1
0	0	0	0	0

Based on Table 4.3, the code word can be written as 11 01 01 11 00. One way of representing the encoder is to specify a set of n connection vectors (generator sequences), one for each of the modulo-2 adders. A 'one' in the generator sequence indicates that the corresponding stage in the shift register is connected to the modulo-2 adder and a zero indicates that no connection exists between the stage and modulo-2 adder. For the encoder example, we write the connection vector g_1 for the upper connection and g_2 for the lower connection as follows:

$g_1 = 1\ 1\ 1$

$g_2 = 1\ 0\ 1$

A convolution encoder is placed before the modulator. At the receiver the decoder detects and corrects error. In the next section we describe Channel decoder.

4.12 Channel Decoding

Channel decoding is used to decode the detected bits and correct errors, if any. A Viterbi decoder is a commonly used channel decoding technique, which uses the Viterbi algorithm for decoding a stream of bits that were encoded based on a convolutional coding. The Viterbi algorithm is the most resource-consuming, but it based on the maximum likelihood decoding [8]. It uses a Trellis diagram [8] for decoding. A trellis is constructed and a metric for every possible path is calculated. The metric for a particular path is defined as Hamming distance [8] between the coded sequence represented by the paths and the received sequence. Thus, for each node in the trellis, the algorithm compares the two paths entering the node. The path with lower metric is retained and other path is discarded.

4.12.1 Example

Suppose the message is 0 0 0 and this message after passing through the convolutional encoder, shown in Figure 4.13 is turned into 0 0 0 0 0 0 0 0 0 0. The coded message is then modulated, up-sampled and filtered. Due to fading effects and AWGN, the demodulated message at the receiver end is 0 0 1 1 0 0 0 0 0 0. The following steps describe the decoding of message using a Viterbi decoder.

Step 1: Paths arrived at level 3 (Figure 4.14)

i) Node 'a' arrived paths	Metric	ii) Node 'b' arrived paths	Metric
00 00 00	2	00 00 11	4
11 10 11	5	11 10 00	3
The survivor path is 00 00 00		The survivor path is 11 10	

iii) Node 'c' arrived paths	Metric	iv) Node'd' arrived paths	Metric
00 11 10	1	11 01 10	4
11 01 01	4	00 11 01	1
The survivor path is 00 11 10		The survivor path is 00 11 01	

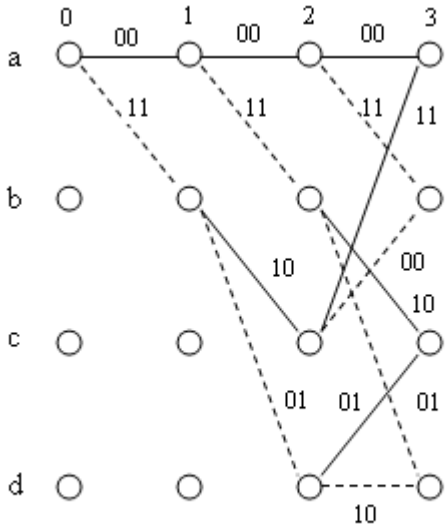

Figure 4.14 Paths arriving at level 3 (Viterbi decoding)

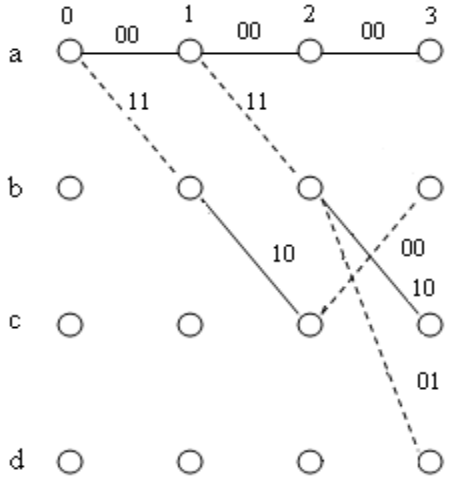

Figure 4.15 Survivor paths at level 3 (Viterbi decoding)

Step2: Paths arrived at level 4

i) Node 'a' arrived paths	Metric	ii) Node 'c' arrived paths:	Metric
00 00 00 00	2	00 11 01 01	2
00 11 10 11	3	11 10 00 10	4

The survivor path is 00 00 00 00 The survivor path is 00 11 01 01

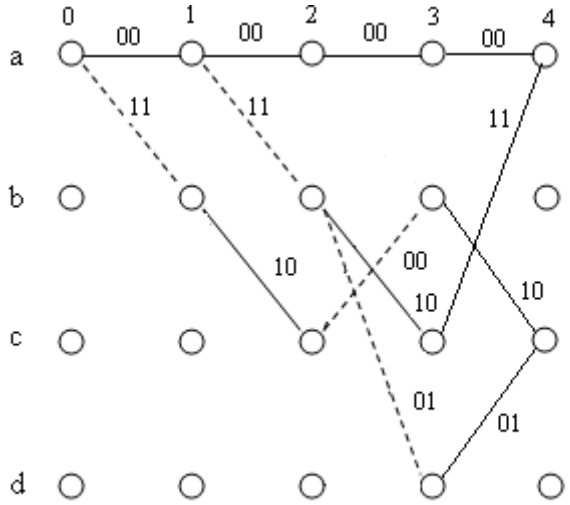

Figure 4.16 Paths arrived at level 4 (Viterbi decoding)

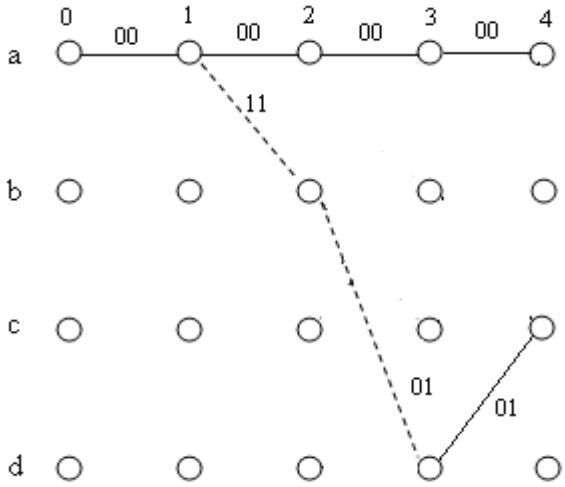

Figure 4.17 Survivor path at level 4 (Viterbi decoding)

Step 3: Paths arrived at level 5:

Node ‘a’ arrived paths Metrics

00 00 00 00 00 2

00 11 01 01 11 4

Therefore the survivor path is 00 00 00 00 00

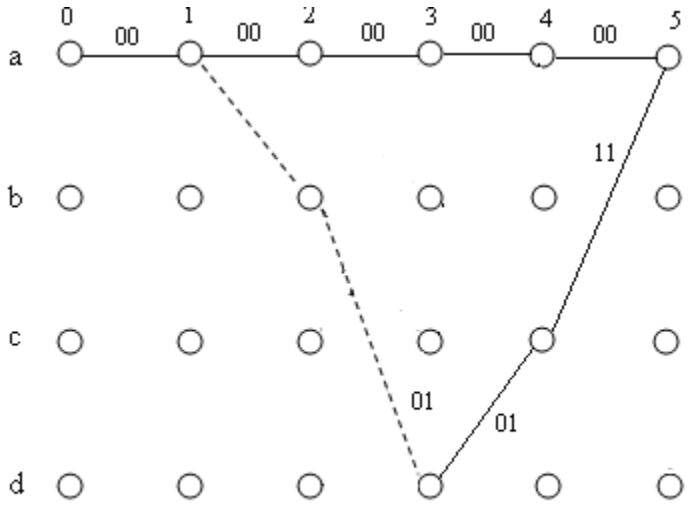

Figure 4.18 Paths arrived at level 5 (Viterbi decoding)

Since there is only one survivor path left, the decoded sequence is 000. Note that the last two bits were ignored because at the encoder side two zero bits were added. Thus, from the above example it can be seen that the Viterbi decoder correctly decoded the demodulated bits.

In our simulation, we created MATLAB code to simulate the channel encoder and decoder and inserted it in our simulated wireless communication system (Figure 4.19).

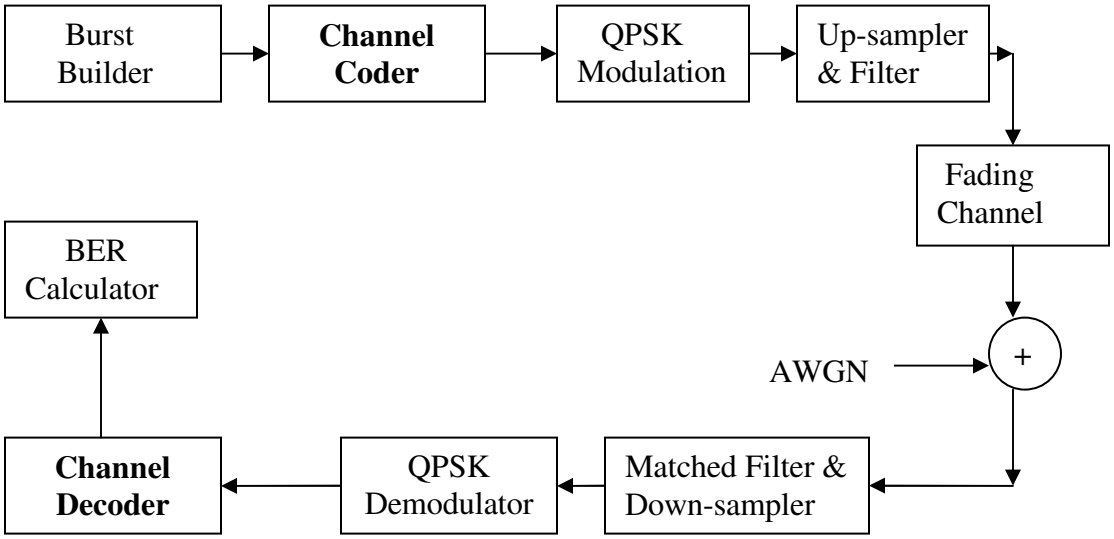

Figure 4.19 Channel coder and decoder incorporated in our simulated wireless communication system

By incorporating channel coding and decoding in a wireless system, the BER with and without the SPB can be measured.

CHAPTER 5

VALIDATION OF THE SPB

5.1 Validation Process

Bit-error-rate testing requires a realistic bit stream representing real audio or speech signal. However, at the stage where we introduce it, that real signal would have been compressed and quantized. Therefore, this sequence can be represented by a random sequence-an i.i.d process. We begin by generating such a sequence of bits (one's and zero's), which we provide as input to the modulator which modulates these bits i.e. convert these bits to symbols. After up-sampling and filtering the signal is transmitted. The up-sampling introduces some correlation in the signal. The effect of fading on signal is incorporated and then WGN in controlled form is added to the signal. This noisy signal then becomes the input to the receiver. The mixture is then passed through the SPB to reduce the effect of noise. Subsequently, down-sampling and filtering are performed. After QPSK demodulation, the BER is calculated and the BER vs. Eb/N0 is plotted. We also run the simulator with channel coding/decoding schemes described in Chapter 4.

Since we are interested in the improvement in the BER, the results are plot of BER vs. Eb/N0.

5.2 Theoretical and Simulated BER Comparison for AWGN Channel

To validate our simulation, a baseline for the comparison purpose was required. The theoretical curve for QPSK with AWGN channel (Figure 4.8, Chapter 4) served as the baseline.

Figure 4.1 was simulated for a burst length of 1000, without fading and the BER was calculated for different values of Eb/N0. Theoretical BER was also calculated using equation (4.33). The simulated and theoretical plots of the BER vs. Eb/N0 were plotted (Figure 5.1). As seen from the plots, the theoretical and simulated curves are almost similar, thus providing some validation that our physical layer simulation of a basic wireless communication system is correct.

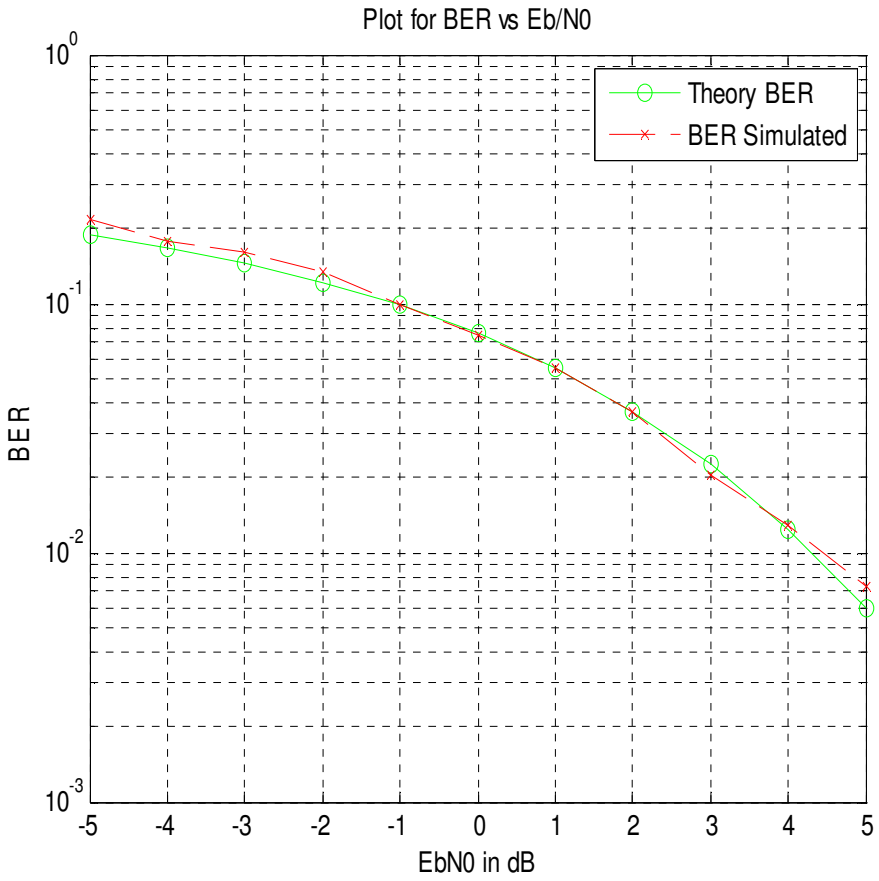

Figure 5.1 Theoretical and Simulated comparison curve.

The values of the BER for different values of Eb/N0 are also shown in Table 5.1. BER Theory gives the theoretical values, using equation (4.33) and BER Simulated gives the simulated values for different Eb/N0.

Table 5.1 Theoretical and Simulated BER

Eb/N0 in dB	-5	-4	-3	-2	-1	0	1	2	3	4	5
BER Theory	.19	.17	.146	.122	.098	.076	.055	.037	.023	.01	.005
BER Simulated	.22	.18	.158	.130	.102	.079	.056	.039	.024	.01	.006

5.3 BER results with our SPB

Figure 4.9, which has the SPB incorporated in a wireless communication system, was simulated (without fading) for a burst length of 1000 bits and the results for the BER for different values of Eb/N0 were calculated. The simulation was also carried out without the SPB and the BER was noted. With the SPB incorporated at the receiver section, the BER improved as shown in Figure 5.2.

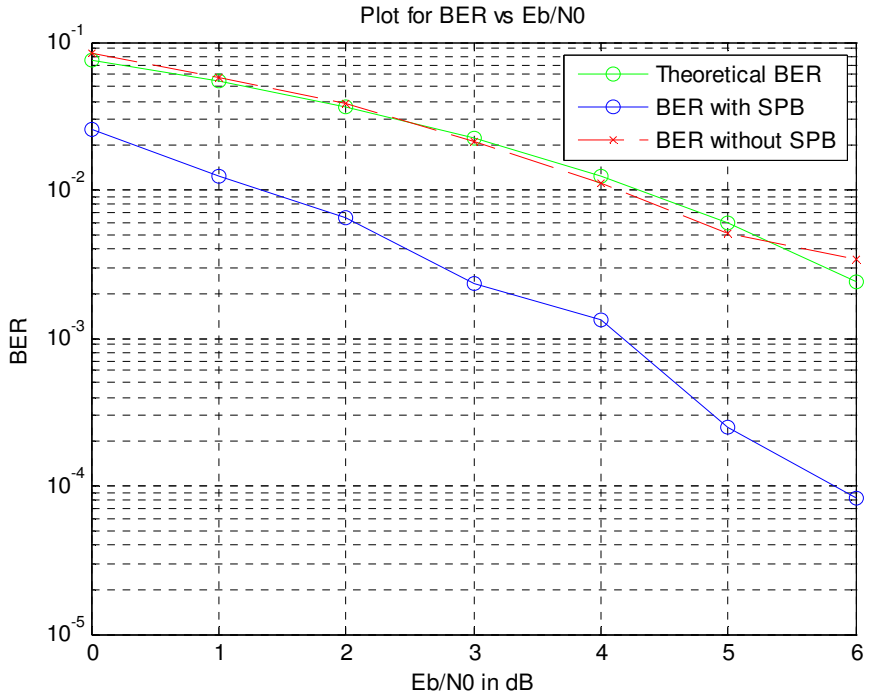

Figure 5.2 BER vs. Eb/N0 with and without the SPB

Table 5.2 shows the results for the BER at different values of Eb/N0. The 'BER Simulated' in the table gives the BER without the SPB. 'BER Signal Processing' on the other hand, gives the result with the SPB.

Table 5.2 BER with and without the SPB

Eb/N0 in dB	0	1	2	3	4	5	6
BER Theory	.0756	.0547	.0368	.0226	.0124	.0059	.0024
BER Simulated	.0783	.0557	.0382	.0250	.0123	.0061	.0027
BER Signal Processing	.0254	.0124	.00658	.0023	.0013	.00025	.00008

From the plot in Figure 5.2 it was observed that a coding gain of approximately 3 dB is obtained.

5.4 BER Results considering the effects of Fading

The previous plot shown in Figure 5.2 did not consider the effect of fading. Ricean fading was modeled using Figure 4.6. The BER curves were plotted for different values of Ricean factor (K).

Figure 5.3 was plotted for $K = 12$, a Doppler shift (fd) of 200 Hz and a burst length of 1000 bits. Figure 5.4 was plotted for $K = 3$, $fd = 200$ Hz and a burst length of 1000 bits. The values of the BER were tabulated for both the cases. It is seen that higher the value of K, lesser will be the effect of fading. The SPB still improves the BER in the presence of fading, irrespective of the values of K.

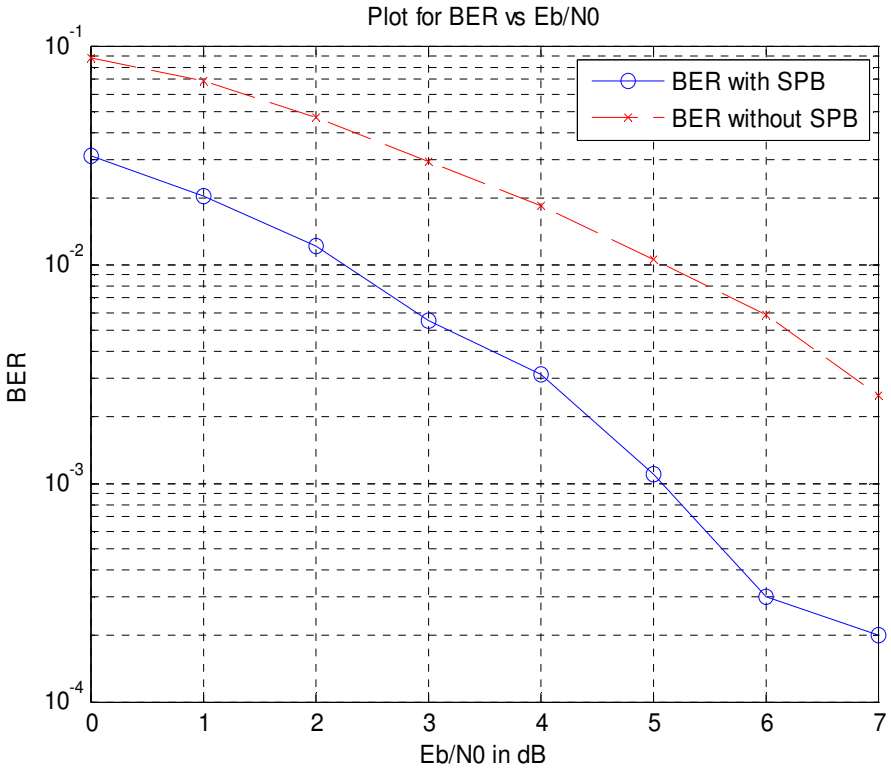

Figure 5.3 BER vs. Eb/N0 with Ricean factor of 12 and Doppler shift of 200 Hz

The tabulated values for BER with different values of Eb/N0 are shown in table below

Table 5.3 BER values with Ricean factor of 12 and Doppler shift of 200 Hz

Eb/N0 (dB)	0	1	2	3	4	5	6	7
BER Simulated	.0883	.0694	.0466	.0296	.0187	.0105	.0059	.0025
BER Signal Processing	.0316	.0205	.012	.0055	.0031	.0011	.0003	.0002

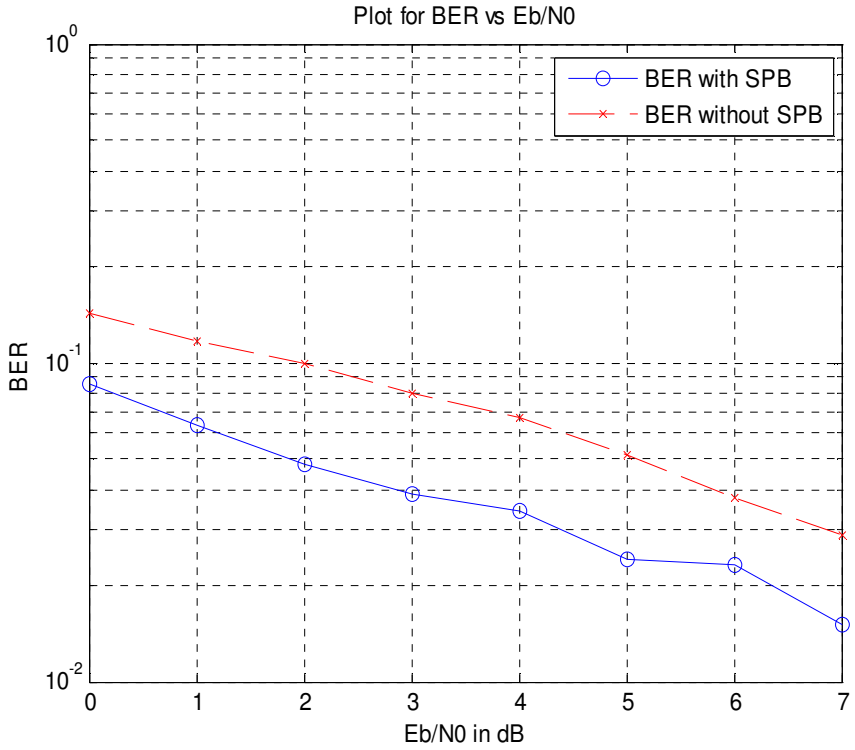

Figure 5.4 BER vs. Eb/N0 with Ricean factor of 3 and Doppler shift of 200 Hz

The tabulated values for BER with different values of Eb/N0 are shown in table below

Table 5.4 BER values with Ricean factor of 3 and Doppler shift of 200 Hz

Eb/N0 in dB	0	1	2	3	4	5	6	7
BER Simulated	.1421	.1161	.0998	.0796	.0669	.0511	.0379	.0287
BER Signal Processing	.0852	.0638	.0477	.0385	.0345	.0242	.0231	.0151

5.5 BER Results with Convolution Coding

All the above plots were without considering the effects of channel coding. Figure 5.5 shows the plot with the coding rate of 1/2. The constraint length taken is 3 and the generator matrix used for encoder design is

$$G = \begin{bmatrix} 1 & 0 & 1 \\ 1 & 1 & 1 \end{bmatrix}$$

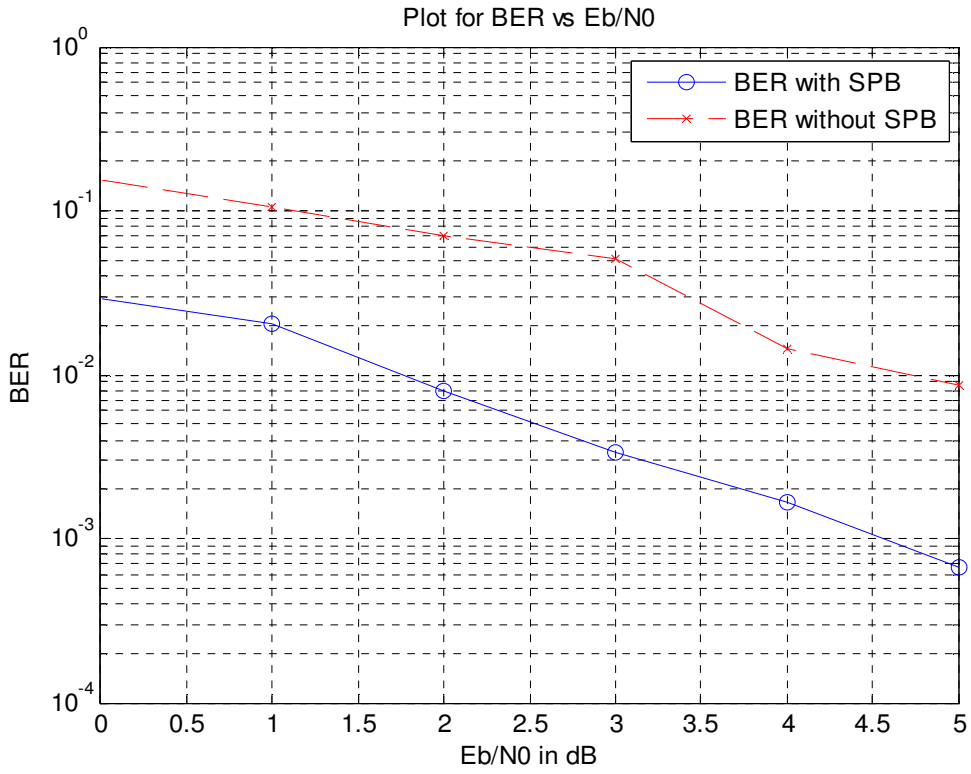

Figure 5.5 BER vs. Eb/N0 with coding rate of 1/2

Even though the Ricean factor of 3 and Doppler shift of 200 Hz are considered, it is seen with the simulation of channel coding/decoding the BER is significantly improved. The use of the SPB with channel coding further reduces the BER. The values of the BER for different values of Eb/N0 is shown in the Table 5.5

Table 5.5 BER values with coding rate of 1/2

Eb/N0 in dB	0	1	2	3	4	5
BER Simulated	.1412	.1055	.071	.0503	.0145	.00867
BER Signal Processing	.0293	.0205	.008	.0033	.00167	.00067

In summary, the BER for different values of Eb/N0 with our SPB can be tabulated as follows:

Table 5.6 Summary table for BER for different values of Eb/N0 with our SPB

Eb/N0 in dB	0	1	2	3	4	5
BER AWGN	.0254	.0124	.00658	.0023	.0013	.00025
BER Fading	.0852	.0638	.0477	.0385	.0345	.0242
BER Coding	.0293	.0205	.008	.0033	.00167	.00067

CHAPTER 6

CONCLUSIONS AND FUTURE WORK

6.1 Conclusions

In this thesis we introduced a novel SPB which may be used for noise reduction in a Wireless Communication System (WCS).

We simulated a transmitter, a channel and a receiver of a WCS. Then, we introduced the SPB at the receiver section and calculated the BER. Based on the simulation results it was concluded that the addition of the SPB at the receiver section *improved the BER*. The BER improvement will:

- help in solving the problem related to call drop outs because of the high BER.
- improve the overall QoS.
- potentially help in the extension of the range of a base station.
- provide a coding gain.

The receiver section of the mobile handsets could incorporate the SPB and improve the call reception quality.

6.2 Future Work

Even though, using simulation results, we have verified the use of the SPB in noise reduction, the real time implications of the SPB needs to be investigated. We carried out the physical layer simulation of a WCS with the SPB incorporated in it, using MATLAB. It took about 5 minutes for the entire simulation to run. Moreover, the SPB

utilizes iterative ‘gradient ascent method’ for noise reduction. Hence, verification should be performed to ensure that this method can be implemented in real time.

We have developed our simulation for a GSM wireless system. This work could be extended to the CDMA systems. The use of the SPB in cell phones requires more investigations. We can also look into the real time chip implementation and/or real-time software of the SPB.

REFERENCES

[1] Derong Liu and Yi Zhang, “A Self-Learning Adaptive Critic Approach for Call Admission Control in Wireless Cellular Networks”, Proceedings of IEEE International Conference on Communications, May 2003, pp.1853-1857

[2] P. Sarath Kumar and Jack Holtzman , “Analysis of Handoff Algorithm using both Bit Error Rate (BER) and Received Signal Strength’’, Proceedings of the 1994 International Conference on Universal Personal Communications, September 1994, pp. 1-5

[3] Huamin Zhu and Kyung Sup Kwak, “An Adaptive Hard Handoff Algorithm for Mobile Cellular Communication Systems”, ETRI Journal, Volume 28, Number 5, October 2006, Page 1

[4] Renyong Wu, Guangxi Zhu, Xiaofeng Lu, Guoqin Ning , “A Predictive Call Admission Control Algorithm for Wireless/Mobile Networks”, IEEE Transactions on Vehicular Technology Conference -2006, Sept. 2006.

[5] Yuguang Fang and Yi Zhang, “Call Admission Control Schemes and Performance Analysis in Wireless Mobile Networks”, IEEE Transactions on Vehicular Technology, Vol 51, March 2002, Page 1-2

[6] David grace, Tim C.Tozer and Alister G.Burr “Reducing Call Dropping in Distributed Dynamic channel Assignment by Incorporating Power Control in Wireless Ad Hoc Networks”, IEEE Journals in selected areas in Communications, Vol 18, November 2000.

[7] Aapo Hyvarinen and Erkki Oja, “Independent Component Analysis: Algorithms and Applications”, Neural Networks Research Centre, Helsinki University of Technology

[8] John G. Proakis,"Digital Communications",Third Edition McGraw-Hill International Editions

[9] Noll, M, "Pitch determination of human speech by the harmonic product spectrum, the harmonic sum spectrum and a maximum likelihood estimate", Proceedings of the Symposium on Computer processing communications, pp 779-797

[10] Cardoso, J.-F, "Infomax and maximum likelihood for blind source separation", Signal Processing Letters, IEEE vol 4, Apr 1997

[11] Kumarabhijeet Singh, "Improving the performance of Wireless system by reducing the BER", MSEE Thesis, University of Texas at Arlington

[12] Theodore S. Rappaport, "Wireless Communications Principles and Practice", Prentice Hall of India, Second Edition

[13] C. Jakes, Jr., *Microwave Mobile Communications*. New York: Wiley, 1974.

[14] Tugay Eyceoz and Alexandra Duel-Hallen, "Deterministic Channel Modeling and Long Range Prediction of fast fading mobile radio channels", North Carolina State University

[15] Don H. Johnson, "Scholarpedia", 2006.

[16] John R. Barry, Edward A. Lee, David G. Messerschmitt," Digital Communications", Third Edition, Kluwer Academic Publishers

[17] Seungjin Choi, "Blind Source Separation and Independent Component Analysis: A Review", Neural Information Processing-letters and review, Vol 6, January 2005

[18] Anthony J. Bell**,** Terrence J. Sejnowski**,** Howard Hughes Medical Institute, Computational Neurobiology Laboratory, The Salk Institute, **"**An Information-

Maximization Approach to Blind Separation and Blind Deconvolution," Neural Computation, 7, 6, 1129-1159

[19] Alberto Leon-Garcia, "Probability and Random Processes for Electrical Engineering", Second Edition, Chapter 6

[20] Qilian Liang, "Non-linear equalization for Ricean Multipath Fading Channel", Acoustics, Speech, and Signal Processing, 2003, Volume 6

BIOGRAPHICAL INFORMATION

The author was born in Amritsar, India on 29th July 1983. He completed his schooling from St. Xavier's High School, Mumbai in 2001. He earned his Bachelor's degree in Electronics and Telecommunication from University of Mumbai, India in May 2005. Thereafter, he pursued Master of Science in Electrical Engineering from University of Texas at Arlington and received his degree in May 2008. During his Master's degree, he worked as a Communication Quality Engineering Intern at The Mathworks.